http://www.kidney-international.org

Podocytes require the engagement of cell surface heparan sulfate proteoglycans for adhesion to extracellular matrices

Shoujun Chen[1], Deborah Wassenhove-McCarthy[2], Yu Yamaguchi[3], Lawrence Holzman[4], Toin H. van Kuppevelt[5,6], A. Wayne Orr[2], Steven Funk[7], Ann Woods[8] and Kevin McCarthy[2,7]

[1]Department of Pathology, University of South Florida, Tampa, Florida, USA; [2]Department of Pathology, Louisiana State University Health Sciences Center, Shreveport, Louisiana, USA; [3]Developmental Neurobiology, Sanford Children's Health Research Center, Sanford-Burnham Medical Research Institute, La Jolla, California, USA; [4]Department of Medicine, School of Medicine, University of Michigan, Ann Arbor, Michigan, USA; [5]Department of Biochemistry, Nijmegen Center for Molecular Life Sciences, Radboud University Nijmegen Medical Center, Nijmegen, The Netherlands; [6]Department of Pediatric Nephrology, Nijmegen Center for Molecular Life Sciences, Radboud University Nijmegen Medical Center, Nijmegen, The Netherlands; [7]Department of Cell Biology and Anatomy, Louisiana State University Health Sciences Center, Shreveport, Louisiana, USA and [8]Department of Cell Biology, School of Medicine, University of Alabama at Birmingham, Birmingham, Alabama, USA

Podocytes adhere to the glomerular basement membrane by cell surface receptors. Since in other cells these adhesions are enhanced by cell surface proteoglycans, we examined the contribution of these molecules and their glycosaminoglycan side chains to podocyte adhesion by developing immortalized podocyte cell lines with (control) or without (mutant) heparan sulfate glycosaminoglycan chains. In adhesion assays control podocytes attached, spread, and migrated more efficiently compared with mutants, indicating a requirement for heparan sulfate chains in these processes. The proteoglycan syndecan-4 is known to have direct effects on cell attachment, spreading, and cytoskeletal organization. We found it localized to focal adhesions in control podocytes coincident with stress fiber formation. In mutant cells, syndecan-4 was associated with smaller focal contacts and cortical actin organization. Analysis by flow cytometry showed that mutant cells had twice the amount of surface syndecan-4 of control cells. Protein kinase Cα, a signaling molecule bound to and activated by syndecan-4, showed a fourfold increase in membrane localization-activation than that seen in control cells. *In vivo*, the loss of heparan sulfate glycosaminoglycans in PEXTKO mice led to a loss of glomerular syndecan-4. Overall, our study provides further evidence for a dynamic role of cell surface heparan sulfate glycosaminoglycans in podocyte activity.

Kidney International (2010) **78,** 1088–1099; doi:10.1038/ki.2010.136; published online 12 May 2010

KEYWORDS: adhesion molecule; cell–matrix interactions; extracellular matrix; glomerular filtration barrier; podocyte

Correspondence: *Kevin McCarthy, Department of Pathology, LSU Health Sciences Center, 1501 Kings Highway, Shreveport, Louisiana 71130, USA. E-mail: kmccar2@lsuhsc.edu*

Received 30 June 2009; revised 12 February 2010; accepted 16 March 2010; published online 12 May 2010

Earlier studies established a paradigm that indicated a role for heparan sulfate proteoglycans (HSPGs) and their glycosaminoglycan chains as critical elements in forming the charge-selective barrier of the glomerular basement membrane (GBM).[1,2] However, several recent reports have challenged that concept, providing compelling evidence to the contrary. Using a molecular genetic approach, two groups have been able to significantly diminish the amount of HSPGs[3] or heparan sulfate (HS) glycosaminoglycans[4] in the GBM with no significant development of proteinuria or albuminuria in the animals. The former study[3] used Cre-lox technology to delete the ability of podocytes to make the core protein agrin, the predominant basement membrane HSPG in the GBM. By doing so, the charge density of the GBM was significantly decreased, because the 'platform' for the assembly of HS chains (for example, the agrin core protein) was absent. In a complementary approach, we used Cre-lox technology to delete the expression of EXT1, a subunit of the HS copolymerase enzyme in podocytes. Taking this approach, we were able to halt the ability of podocytes to assemble HS chains on all proteoglycan core proteins synthesized by podocytes. PEXTKO (podocyte-specific *EXT1* knockout) mutant mice have GBMs with a significant decrease in the amount of HS glycosaminoglycans similar to that reported by Harvey *et al.*[3] Both studies used polyethlyeneimine staining at the ultrastructural level to clearly show a significant decrease in anionic charge density within the GBM, the majority of the polyethlyeneimine staining remaining on the endothelial side of the basement membrane. Our report, however, showed foot process effacement of the podocytes at all ages examined, whereas in the model of Harvey *et al.*[3] these changes were not observed. This unique observation led us to speculate that the HS deficiency influenced the microenvironmental sensing pathway in

podocytes mediated by cell surface proteoglycans and their associated HS. In other cell systems, members of the syndecan cell surface proteoglycan family, have been shown to have direct effects on mediating cell–matrix interactions. Within that family, syndecan-4 has been shown to have direct effects on cell attachment, spreading, and cytoskeletal organization.[5,6] Although an earlier study had reported the presence of syndecan-4 in the glomerulus,[7] the study focused exclusively on mesangial cell biology. A recent report[8] showed the presence of syndecans-1 and -4 on podocytes in normal renal tissue sections.

This study reports the start of our investigation into the role of HS and cell surface HSPGs in mediating podocyte–matrix interactions. For the purposes of this study, we are using the well-described patterns of syndecan-4 staining during cell adhesion as a readout to allow us to show that HS attached to cell surface proteoglycans are important co-receptors alongside integrins in podocyte–matrix interactions. Loss of the HS chains alters the ability of podocytes to interact with their local microenvironment, causing significant decreases in their ability to attach, spread, and migrate on extracellular matrices. These behaviors have part of their genesis in the negative effects of lack of cell surface HS on the organization of podocyte focal adhesions, the cell surface localization of syndecan-4, and the arrangement of the podocyte actin cytoskeleton. Furthermore, our study reports a novel finding that in non-confluent HS− cells there is an increase in the cell surface abundance of syndecan-4 core protein. This correlates with an enhanced cell membrane localization/activation of Protein Kinase C (PKCα), a key signaling intermediate in syndecan-4-mediated stress fiber formation. However, in confluent cells and *in vivo* the opposite occurs with regard to syndecan-4 abundance, there is ostensibly less syndecan-4 staining in the HS− cells compared with the HS+ cells.

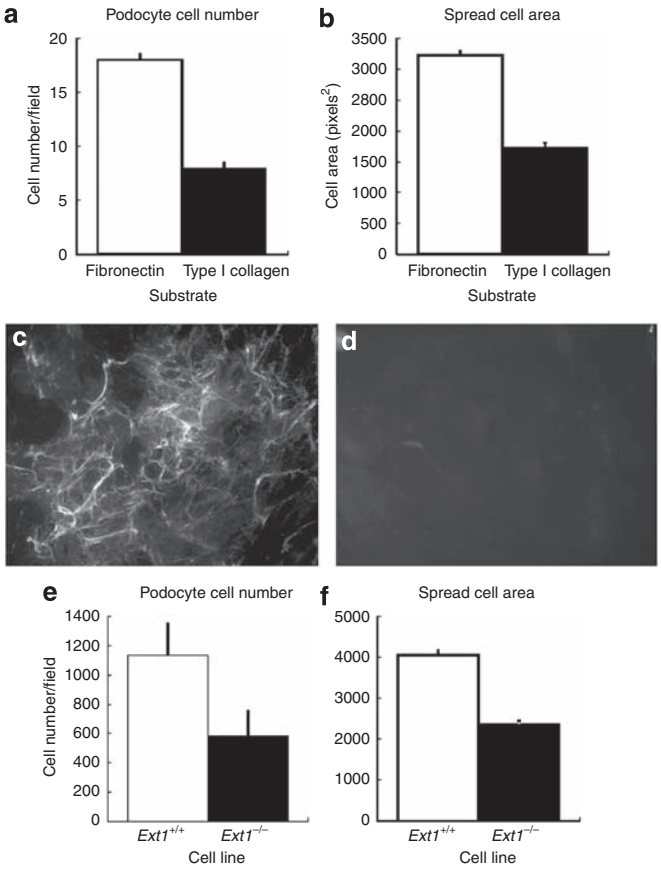

Figure 1 | Podocytes use cell-surface heparan sulfate proteoglycans (HSPGs) for cell–matrix interactions. To initially analyze the possibility that the cell surface HS may have a role in podocyte attachment, adhesion assays using *EXT1*$^{+/+}$ podocytes were run using substrata consisting of either monomeric type I collagen or plasma fibronectin. The data show that podocytes attach (**a**) and spread (**b**) ($P<0.0001$) less efficiently on monomeric type I collagen compared with fibronectin. The micrographs shown in (**c**) and (**d**) are of immortalized *EXT1*$^{fl/fl}$ podocytes (**c**) that were infected by adenoviral-mediated gene transfer with constructs of Ad-green fluorescent protein (GFP) (HS+ podocytes) or (**d**) GFP-Cre recombinase (HS− podocytes). The images show the cells from cultures of both lines 48 h after seeding. Panel (**c**) shows HS4C3 staining (anti-HS) of the HS rich extracellular matrix laid down by podocytes during the timeframe. In the Cre-recombinase-transfected cells (**d**), there is no staining by HS4C3 at either the cell surface or the pericellular matrix. (Final magnification ×200, the exposure time for both panels was held constant.) The graphs in Figure 2e and f shows that the loss of cell surface HS (*EXT1*$^{-/-}$) in podocytes results in a significant decrease in cell adhesion (**e**, $P<0.01$) and spread cell area (**f**, $P<0.0001$) compared with control cells (*EXT1*$^{+/+}$).

RESULTS

To develop an understanding of how cell surface HS might affect podocyte adhesion, we first compared the ability of immortalized wild-type podocytes to adhere to fibronectin or monomeric type I collagen in short-term (4 h) adhesion assays. Fibronectin was chosen because it is known to support focal adhesion formation, which is integrin- and syndecan-4 dependent.[9] Monomeric type I collagen, the other substratum used in the assay, does not bind HS as efficiently as type I collagen heterotrimer[10] but still does permit cell adhesion. In such adhesion assays, podocytes adhered to- and spread less efficiently to monomeric type I collagen substrates compared with fibronectin substrates (Figure 1a and b; $P<0.0001$) suggesting that cell surface HS might have a critical role in mediating podocyte–matrix interactions. To further test this premise, a line of immortalized podocytes containing the *Ext1*$^{fl/fl}$ allele was developed and then Cre-mediated excision of the allele was carried out *in vitro* through adenoviral transduction. The resultant podocyte cell lines (HS+ or HS−; Figure 1c and d). were immunostained with antibody HS4C3, which recognizes 3-O-sulfated carbohydrate epitopes on HS secreted by podocytes.[11] HS4C3 staining showed that HS+ podocytes assembled a dense pericellular matrix (Figure 1c) that was absent in the HS− podocyte cell cultures. Thus, the lack of HS4C3 staining showed that the ability to assemble HS was lost in the HS− cells (Figure 1d). Using HS+ and HS− podocyte cell lines, we then analyzed whether or not the lack of HS− would compromise the ability of podocytes to attach and spread on

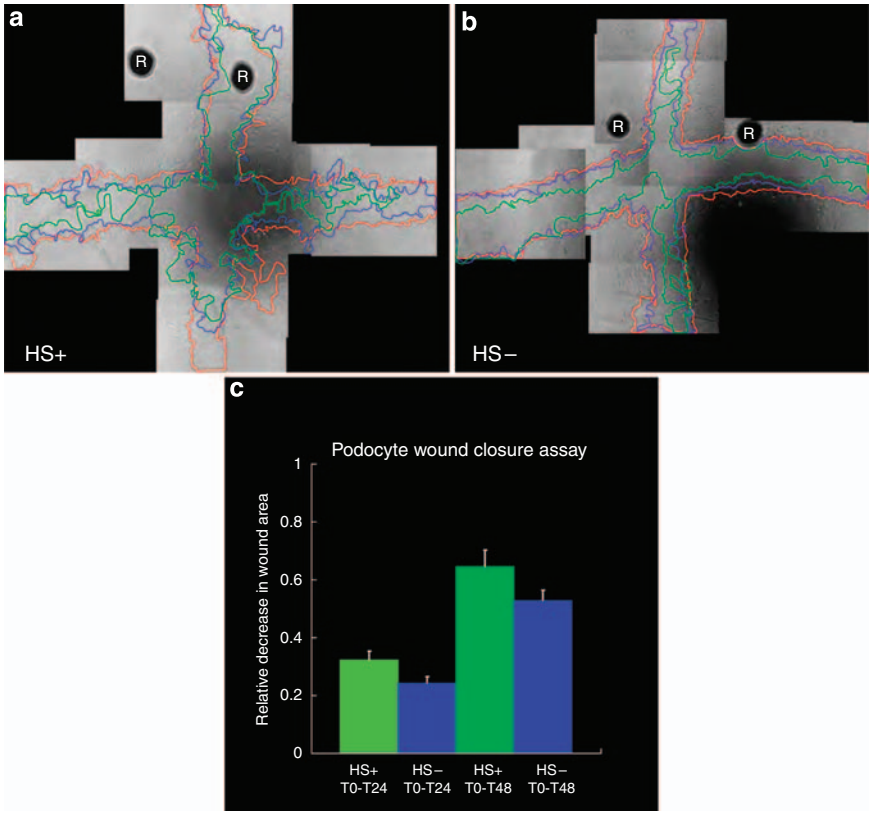

Figure 2 | Loss of cell surface heparan sulfate (HS) delays podocyte cell migration in a scratch wound assay system. Confluent monolayers of HS+ (**a**) or HS− (**b**) cells grown in 24-well plates were scratch-wounded in a crosswise manner using a pipette tip. Registration marks (R in micrographs) were etched into the bottom side of the plate to facilitate later image alignments during the course of the study. The progress of cell migration into the denuded area tracked over time using phase contrast microscopy. Images were taken of the boundaries of the wound areas at $T=0$ (red line), $T=24$ (blue line), and $T=48$ (green line) and the leading edges of the cell migration traced using image analysis software (final magnification ×100). The area for each scratch wound was calculated using a planimetry subroutine in the image analysis software and the relative change in area from $T=0$ was determined using the equation $\frac{[A_o-A_n]}{A_o}=\Delta A$, where A_0 = area at $T=0$, A_n = area at Time = n, and ΔA is the relative change in area. (**c**) is the bar graph depicting the relative change in the wound area as a function of time. At both times ($T=24$, 48) the HS+ cells showed a greater efficiency (0.32 for HS+ vs 0.24 for HS− at $T=24$; 0.65 for HS+ vs 0.53 for HS− at $T=48$) for wound closure ($P<0.006$ for $T=24$ h, $P<0.03$ $T=48$ h).

a fibronectin substratum in short-term adhesion assays. HS− podocytes showed diminished adhesion efficiency ($P<0.01$, Figure 1e) and smaller spread cell areas ($P<0.0001$, Figure 1f) when compared with HS+ podocytes.

As cell surface HS has been shown to be critical in cell migration, we used a scratch wound assay to measure differences in the ability of HS+ and HS− podocytes to migrate into the wounded area (Figure 2). HS+ podocytes (Figure 2a) closed the wound more efficiently than their HS− counterparts (Figure 2b). Comparing timecourse measures ($T=24$, 48 h post-wounding) of the leading edge of the cells have shown that the HS+ cells migrated into the wound area with a significantly greater efficiency ($P<0.006$ for $T=24$ h, $P<0.03$ $T=48$ h) than the HS− cells (Figure 2c).

As syndecan-4 has been shown to modulate focal adhesion formation in other cell systems, HS+ and HS− cells were seeded into fibronectin-coated microwell chambers and allowed to interact with the substratum for 4 h before fixation and immunostaining for syndecan-4. In HS+ cells that were well spread, large focal clusters of syndecan-4-positive immunoreactivity were observed on the periphery of the cells (Figure 3a and c, arrows). In comparably spread HS− cells, the clustering of syndecan-4 in HS− cells was variable, more often than not appearing as smaller, punctate staining around the periphery of the cell (Figure 3d and f, arrows). Differences in the organization of the cytoskeleton were also observed between the HS+ and HS− podocytes, the HS+ podocytes having prominent stress fibers (Figure 3b and c) whereas HS− podocytes showed the presence of cortical actin organization (Figure 3e and f). To further analyze how the loss of cell surface HS affected cell adhesion, double-label immunofluorescence of HS+ and HS− podocytes using antibodies directed against syndecan-4 and vinculin was carried out, because colocalization of the two molecules would be indicative of focal adhesion formation.[12] In HS+ podocytes, syndecan-4 staining was observed at filipodia at the periphery of the cell (Figure 3g, arrows), its pattern of immunofluorescence colocalized with that of vinculin (Figure 3h and i, arrows). In HS− podocytes (Figure 3j–l), the degree of colocalization was diminished

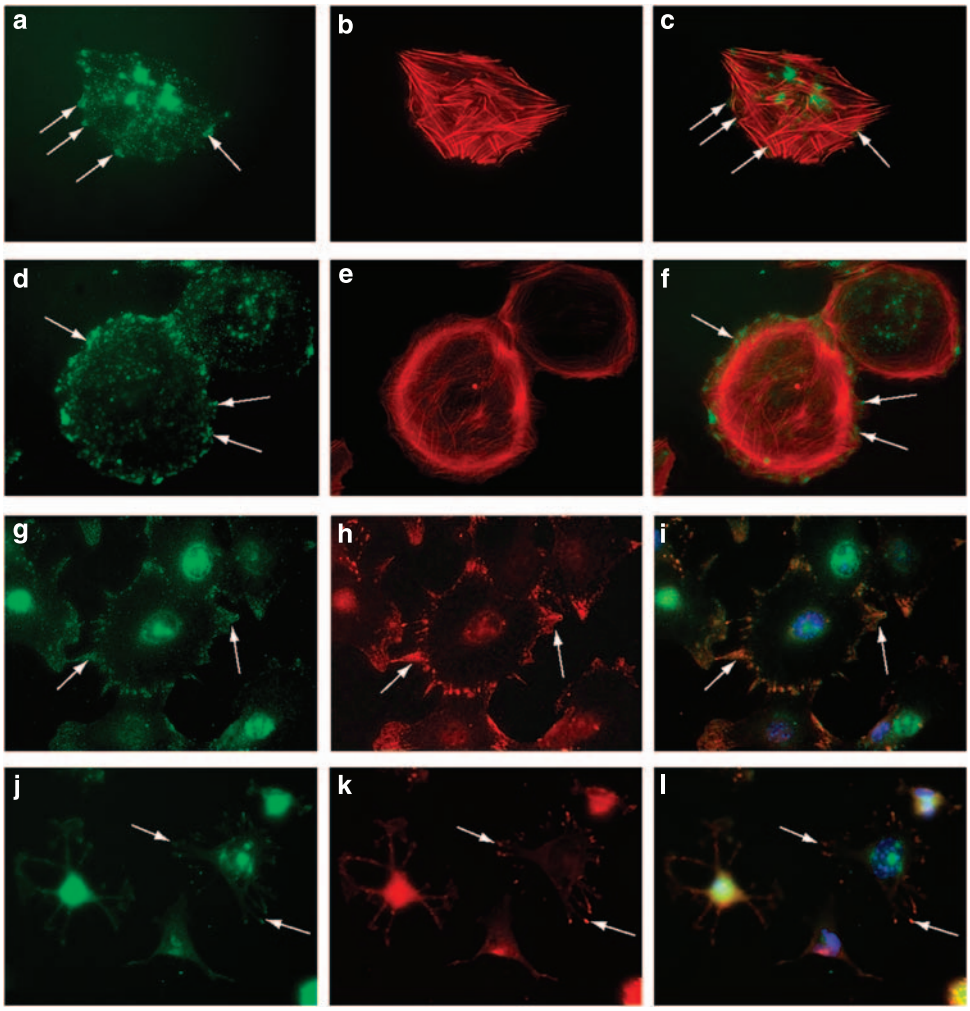

Figure 3 | Loss of heparan sulfate (HS) in podocytes affects cytoskeletal organization and focal adhesion assembly in podocytes in short-term adhesion assays. Podocytes were seeded at low density (10K cells per well) on a fibronectin substratum for 4 h). The cells were double-label immunostained with antibodies directed against syndecan-4 (**a**, **d**, **g**, **j**, green) or vinculin (**h**, **k**, red) or the actin cytoskeleton stained with fluorchrome-conjugated phalloidin (**b**, **e**, red). Hoechst 33242 nuclear stain was used as a nuclear counterstain in some cultures. (**c**, **f**, **i**, **l**) are the digital overlay images for each respective row. HS+ podocytes stained showed prominent stress fibers (**b**), some of which appeared to terminate in large, discrete clusters of syndecan-4 (**a**, arrows). Cortical actin was observed (**e**) in HS− podocytes that were able to spread onto the fibronectin substrate. Syndecan-4 staining in these cells (**d**) appeared as small punctate but more numerous clusters around the periphery of the cell (arrows). In HS+ cells that were actively spreading (**g–i**), syndecan-4 staining (**g**) colocalized with vinculin staining (**h**) in cell processes (arrows); some actively spreading podocytes that were HS− (**j–l**) had multiple thin processes extending from the cell body, the termini of which showed colocalization for vinculin (**k**) and syndecan-4 (**j**, arrows). (Final magnification ×400.)

(arrows). Some of the attaching podocytes were not as well spread as HS+ podocytes and possessed long, attenuated processes, the ends of which showed immunoreactivity for both syndecan-4 and vinculin.

Previous reports in other cell systems have shown that the cytoplasmic tail of syndecan-4 binds to α-actinin[13–15] and PKCα,[16–18] localizing these molecules to areas of focal adhesions. To analyze if podocytes followed a similar paradigm, HS+ and HS− podocytes were double-label immunostained for syndecan-4 (Figure 4a, d, g and j) and α-actinin-4 (Figure 4b and e) or PKCα (Figure 4h and k). In cells actively sending out lamellipodia (Figure 4a–c, double arrows), α-actinin-4 and syndecan-4 were colocalized immediately behind the leading edge of the lamellipodium (double arrows). In cells with well-developed adhesions (Figure 4a–c, arrowheads), colocalization of syndecan-4 and α-actinin-4 was still observed, albeit the localization was diffuse when compared with that observed in the lamellipodia. Within some of these adhesion sites, α-actinin-4 staining had a linear path, presumably dictated by the formation of actin stress fibers, extending in a retrograde manner from the leading edge (Figure 4b, small arrows). These structures were not organized to a similar extent in the HS− podocytes (Figure 4d–f). A similar pattern of colocalization with regard to syndecan-4 and PKCα was observed within the lamellipodia of spreading podocytes in HS+ cells (Figure 4g and h).

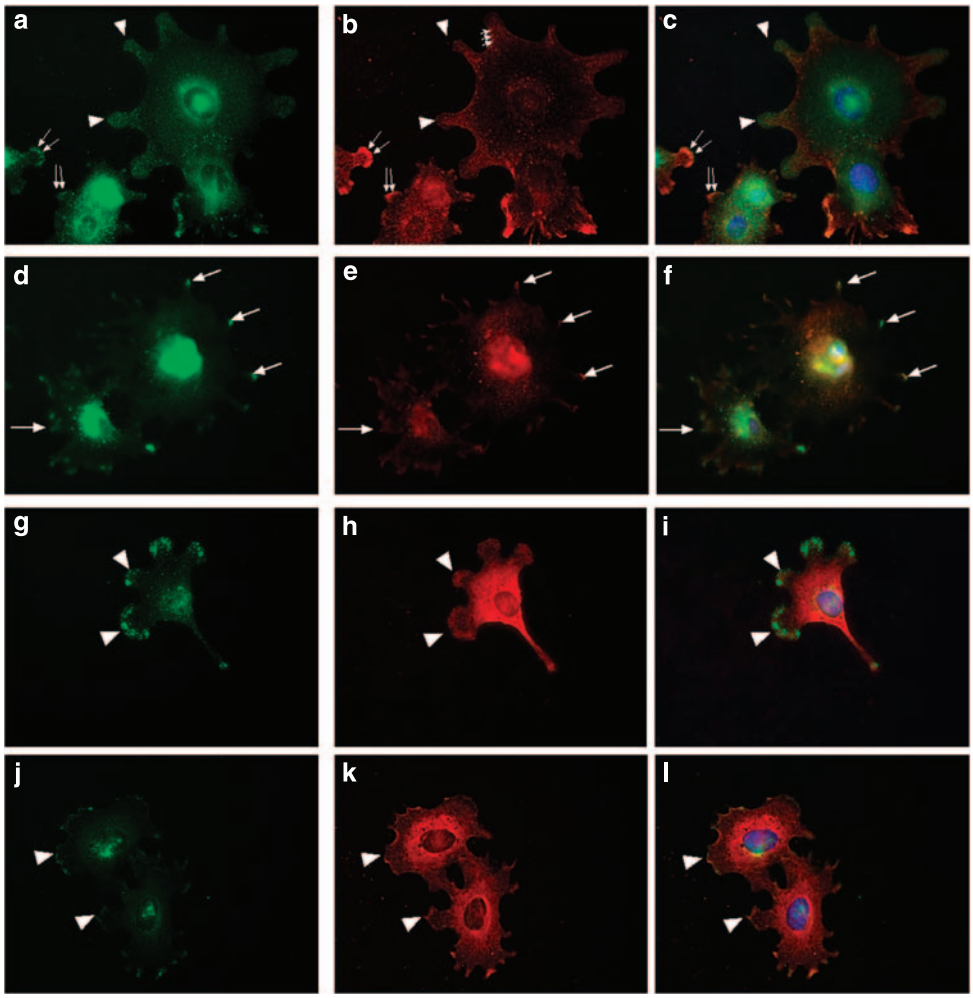

Figure 4 | The pattern of localization of known syndecan-4-binding proteins is altered in heparan sulfate (HS)-GAG− podocytes. The lamellipodia of actively spreading HS+ podocytes showed large, discrete clustering of syndecan-4 (**a**, arrowheads), some of which colocalized with α actinin-4 staining (**b**, arrowheads). Staining for α actinin-4 also appeared as fibrils radiating from the areas of syndecan-4-positive lamellipodia (**b**, smaller arrows) toward the center of the cell. In cells that appeared to be in the earlier stages of lamellipodia extension both syndecan-4 and -actinin-4 were colocalized at the leading edge (**a**, **b**, larger arrows). In HS− podocytes (**d**), syndecan-4 stained the ends of small processes (arrows) and colocalized with α actinin-4 (**e**, arrows) in these processes. Protein kinase Cα (**h**) staining was observed at the leading edges of lamellipodia (arrowheads), colocalized with syndecan-4 (**g**, arrowheads) in HS+ podocytes (**g–i**). In HS− podocytes (**j–l**) both PKCα (**k**) and syndecan-4 (**j**) were colocalized (arrowhead) in small membrane ruffles and small processes extending from the cell body. (Final magnification ×400.)

HS− podocytes showed smaller, ruffled borders that radiated from all edges of the cell with significantly diminished localization of either molecular species at the leading edge (Figure 3j–l).

The morphology data shown in Figure 3d suggested that perhaps the HS− cells might possess more syndecan-4 core protein on their surfaces when compared with HS+ podocytes (cf Figure 3a), albeit the syndecan-4 staining is predominately concentrated in larger clusters or 'pods' in HS+ cells. To further analyze this observation, short-term suspension cultures (2 h) of both HS+ and HS− podocytes were immunostained for syndecan-4 using a phycoerythrin-conjugated syndecan-4 ectodomain antibody and the relative levels of cell surface syndecan-4 measured by flow cytometry (Figure 5). The data show that the HS− podocytes have twice the amount of syndecan-4 staining per cell on their surfaces compared with HS+ podocytes ($P<0.0001$), which might assist their ability to attach to the substratum (Figure 5b). However, even at the 2-h time interval the HS− podocytes do not spread as efficiently as wild-type cells (cf-Figure 5a).

Given the fact that the variable region of the cytoplasmic domain of syndecan-4 is capable of binding to PKCα, one might predict that concomitant with the net increase in cell surface syndecan-4 levels in HS− podocytes an increase in the amount of membrane-bound fraction of PKCα would occur in HS− podocytes. The data in Figure 6a show an approximate fourfold increase ($P<0.001$ compared with control) in the amount of PKCα localized to the membrane-bound fractions of HS− podocytes that were in the process of developing cell–matrix contacts when compared with that of

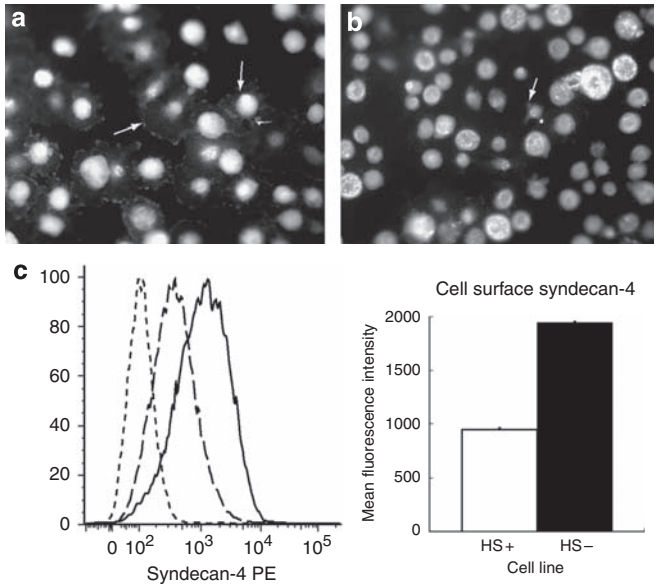

Figure 5 | The expression of syndecan-4 is upregulated in heparan sulfate (HS)− podocytes when compared with HS+ podocytes. (a and **b)** show HS+ (**a**) and HS− (**b**) podocytes immunostained syndecan-4 in the process of adhesion to fibronectin-coated (100 μg/ml) substratum at $T = 2$ h. The HS+ podocytes have attached and spread, the arrows (white) indicating focal clusters of syndecan-4 immunoreactivity at the leading edges of the cells. The HS− podocytes during the same time interval have attached but are poorly spread, the arrows indicating small processes extending from the round cell body. (Final magnification ×200.) The graph and chart in **c** represent the results of flow cytometry studies. The graph shows three traces: non-immune antibody control ----------, HS+ cells stained for syndecan-4 ——— —, and HS− cells stained for syndecan-4 _____. The chart shows the relative fluorescence intensity values for syndecan-4 staining in HS+ and HS− cells. The data show a net increase in the staining for syndecan-4 in HS− cells.

wild-type controls. No significant differences were observed in the between the two groups for intracellular, non-membrane-bound PKCα (Figure 6b).

Although the cell adhesion assays provided information regarding the effects of HS loss on cell attachment and spreading on extracellular matrices, the assays only examined cells that were unilaterally interacting with extracellular matrix in a subconfluent state. However, *in vivo* podocytes interact with other podocytes and the GBM matrices. To determine the effects of loss of HS on confluent podocytes, confluent aggregates were examined with regard to syndecan-4 and PKCα localization. Syndecan-4-positive immunoreactivity was observed at the areas of cell–cell contact of confluent HS+ podocytes (Figure 7b), outlining the perimeter of each cell. PKCα staining (Figure 7a) followed the same pattern of staining as observed for syndecan-4. In contrast, rather than the linear staining at areas of cell–cell contacts observed in the wild-type cells, both syndecan-4 (Figure 7e) and PKCα (Figure 7d) were localized as irregularly spaced clusters of positive immunoreactivity around the perimeter of the HS− podocytes.

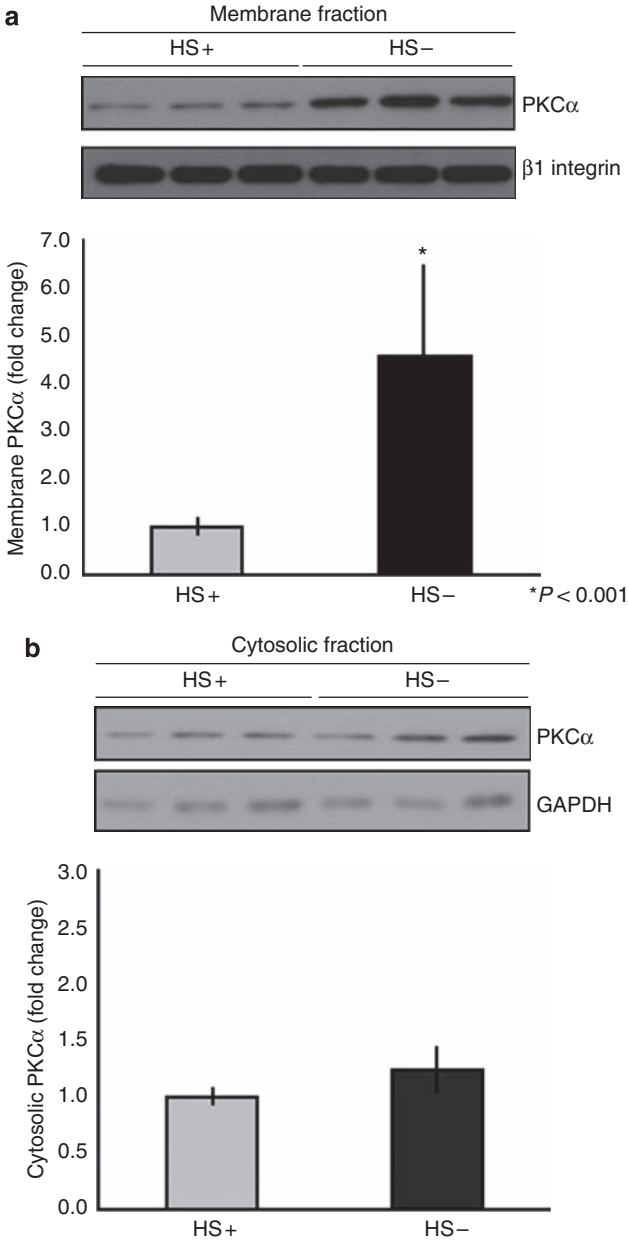

Figure 6 | The membrane localization of PKCα is significantly enhanced in heparan sulfate (HS)− podocytes when compared with HS+ podocytes. Isolated membrane (**a**) and cytosol (**b**) fractions from HS+ and HS− podocytes were separated by sodium dodecyl sulfate-polyacrylamide gel electrophoresis (SDS-PAGE) and the respective pools analyzed by western blot immunoassay using antibodies recognizing PKCα. The blot was subsequently reprobed with antibodies against β1 integrin (for cell membranes) or glyceraldehyde 3-phosphate dehydrogenase (for cytosol) as a normalization control. The graph below shows the results of densitometric scanning of the blot, the PKCα membrane localization/activation significantly greater ($P < 0.001$) in the HS− cells compared with the HS+ cells. In contrast, there were no significant differences between the two cell populations with regard to cytosolic levels of PKCα.

Our earlier studies have shown that the podocytes in PEXTKO animals developed foot process effacement by 30 days postnatal, persisting well into adulthood.[4] To correlate

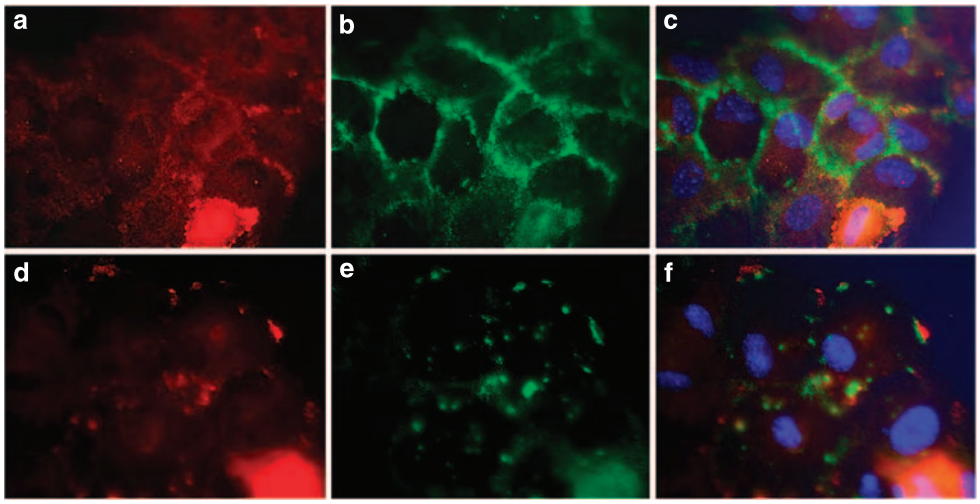

Figure 7 | Loss of heparan sulfate (HS)-GAGs in podocytes alters the distribution of syndecan-4 and PKCα in confluent monolayers of podocytes. Podocytes were seeded at high density (25K cells per well) on a fibronectin substratum. After fixation and permeablilization the cells were immunostained with antibodies directed against syndecan-4 (**b**, **e**) and PKCα (**a**, **d**). (**c**, **f**) represent digital overlays of the images in their respective rows. The images show that in the HS + cells syndecan-4 and PKCα colocalize in a linear pattern at the edges of cells in which cell–cell contact is made (**a**–**c**). In HS− podocytes (**d**–**f**), the peripheral localization of PKCα and syndecan-4 was entirely disrupted, only focal clusters of colocalization are observed. (Final magnification × 400.)

the present *in vitro* studies with *in vivo* observations, we immunostained tissue sections from kidneys of control (HS +) and PEXTKO (HS−) mice with the anti-ectodomain syndecan-4 monoclonal antibody (Figure 8). As the syndecan-4 core protein is almost ubiquitously expressed, we counterstained podocytes with a polyclonal antiserum raised against synaptopodin (Figure 8b, d, f and h). For comparative purposes, tissue sections from podocyte-specific agrin knockout mice (*2.5PCre/Agrn*$^{fl/fl}$) or control (*2.5PCre/Agrn*$^{fl/+}$). These animals also have significantly decreased levels of basement membrane HS because of a podocyte-specific knockout of agrin, but foot process effacement was shown not develop in these animals.[3] In glomeruli from control animals from both murine strains syndecan-4 immunostaining had a punctate appearance (Figure 8a and c) along the outer border of the glomerular capillary walls. The syndecan-4 staining localized along the same plane with the synaptopodin staining, but did not always show precise colocalization in all areas with synaptopodin (Figure 8b and d). In PEXTKO animals (HS−), the dominant pattern of punctate staining for syndecan-4 along the glomerular capillary walls was lost (Figure 8e), the residual immunostaining observed in the mesangium and a minor amount of subendothelial staining. In contrast to the staining observed in the PEXTKO animals, staining for syndecan-4 remained unchanged in the podocyte-specific agrin knockout mice (Figure 8g, *2.5PCre/Agrn*$^{fl/fl}$). The staining density for synaptopodin in the glomeruli from PEXTKO animals (Figure 8f) appeared more diffuse when compared with the more compact staining density observed in the glomeruli from the *2.5PCre/Agrn*$^{fl/fl}$mouse (Figure 8h).

DISCUSSION

The data from the present studies show that cell surface-associated HS glycosaminoglycans have a critical role in mediating the behavior of podocytes during their interactions with extracellular matrices. This report assigns new role for cell surface proteoglycans and HS as direct modulators of podocyte behavior. Cells lacking surface-associated HS attached and spread less efficiently on extracellular matrices and had less efficient migration compared with their wild-type counterparts. The consequences of the absence of HS extend into alterations of cytoskeletal organization and at least one signaling pathway associated with cell-matrix adhesion. As HS are always found covalently attached to proteoglycan core proteins, the number of candidate cell surface proteoglycan core proteins that possibly mediate these events are relatively few-primarily members of the syndecan and/or glypican family. In this study, we chose to examine the potential changes in the pattern of distribution of syndecan-4, because it has been shown in other cell systems to function as an adhesion co-receptor along with integrins by facilitating the ability of the cells to attach and spread on extracellular matrices. Consistent with the syndecan-4 knowledge base, in this present report we show that HS promotes the localization of syndecan-4 to focal adhesions in podocytes and are important mediators in syndecan-4 clustering in these cells.

Previously, we showed that targeted deletion of the *Ext1* gene let to significant loss of HS abundance in the GBM and significant depletion of charge density was observed in the lamina rara externa immediately subtending the pedicels.[4] Podocyte foot process effacement coincided with loss of charge from the lamina rara externa, suggesting the probability that *in vivo* cell surface HSPGs serve as adhesion co-receptors. When functioning in this capacity, one would surmise that cell surface HS would be clustered around the base of podocyte foot processes. In the case of confluent podocytes in culture, the sites of cell–cell contact are thought to be the *in vitro* parallel of pedicels and, in our study,

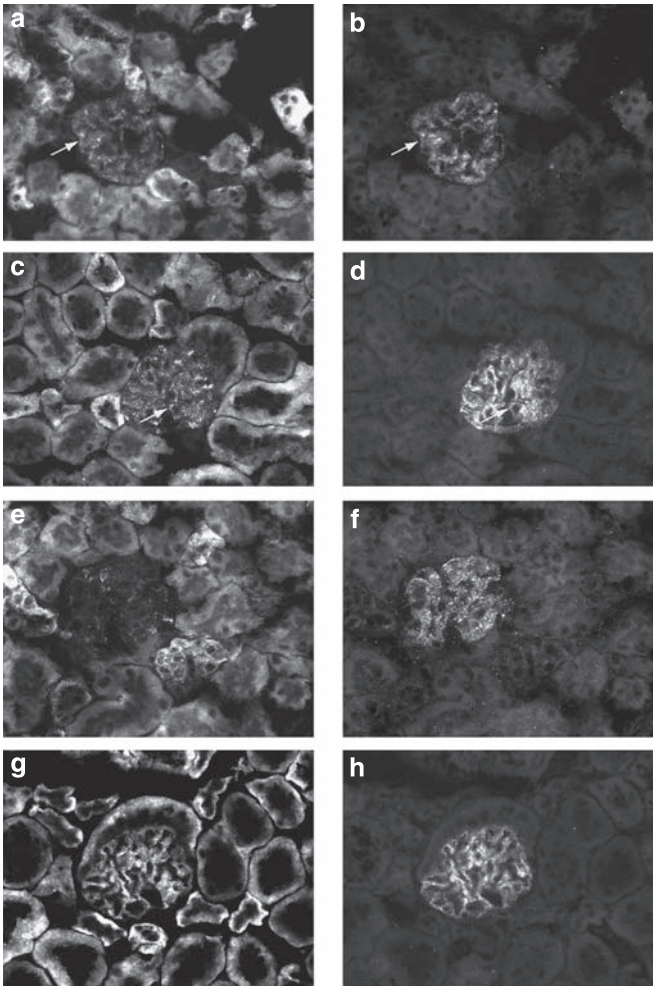

Figure 8 | Podocytes make syndecan-4 *in vivo*. The micrographs in Figure 8 are sections of kidney immunostained for syndecan-4 (**a**, **c**, **e**, **g**) and for synaptopodin (**b**, **d**, **f**, **h**). (**a**, **b**) are glomeruli from controls (heparan sulfate (HS) +) 2.5PCre-*Ext1*$^{+/+}$ animals; (**c**, **d**) are glomeruli from controls (agrin +) 2.5PCre-*Agrn*$^{+/fl}$ animals. In both control groups, syndecan-4 (**a**, **c**) immunostaining within the glomerulus is seen as a punctate pattern that colocalizes (arrows) in part with synaptopodin (**b**, **d**). The same pattern of localization is also maintained in the 2.5PCre-*Agrn*$^{fl/fl}$ mice (**g**), whose podocytes are unable to make the full-length core protein of agrin. In contrast, the punctate pattern of syndecan-4 immunostaining is severely diminished in the glomeruli from the 2.5PCre-*Ext1*$^{fl/fl}$ mice (**e**) (final magnification ×400).

syndecan-4 and its associated HS localizes with those areas (Figure 7). Although the experiments in this study do not use ultrastructural approaches to directly test this concept, the data from this study and the recent report by Cevikbas *et al.*[8] show that podocytes have syndecan-4 on their cell surfaces and the images in this present report (Figure 8) further corroborate their observations.

The existence of podocyte cell surface proteoglycans has one aspect of its genesis from observations in earlier works of Kanwar and Farquhar.[1,19] In their seminal studies in this area, they showed that some of the anionic charge in the GBM (by ruthenium red staining) was connected to the epithelial cell membranes by fine filaments[1] and subsequently identified the anionic species in this region as HS. However, because the existence of cell surface-associated proteoglycans was not recognized until several years later,[20,21] the anionic charge in the lamina rara externa had been attributed to basement membrane HSPGs such as agrin and perlecan. Given the recent suggestion by others that syndecan HS could extend beyond the cell surface up to 500 nm,[22,23] it would be very likely that some of the filamentous material that first observed by Kanwar and Farquhar[1] were the HS chains of syndecan proteoglycans stained by the ruthenium red technique.

The data in this present report further bolster the concept that the HS on cell surface proteoglycans has other functions that differ from the HS of the basement membrane proteoglycans. The loss of HS from basement membrane proteoglycans seems to have little effect on overall podocyte behavior in either the *2.5PCre/Agrn*$^{fl/fl}$mouse[3] or, more recently, in the double mutant mouse, *2.5PCre/Agrn*$^{fl/fl}$ *HSPG2*$^{\Delta 3/\Delta 3}$,[24] because foot process effacement was not reported in either model of basement membrane HS deficiency. If indeed cell surface proteoglycans through their HS chains serve a critical function as a podocyte adhesion co-receptor that influence of foot process organization then the latter would be anticipated, especially in light of the fact that the GBM has multiple redundant ligands capable of binding HS and engaging cell surface proteoglycans, including laminin, type IV collagen, and even plasma fibronectin that gets trapped in the GBM.[25]

The localization of syndecan-4 to focal adhesions in podocytes represents the identification of yet another segment of the signaling/scaffolding nexus in podocytes promoting cell adhesion and spreading. In a manner similar to integrins, the cytoplasmic tail of syndecan-4 is devoid of inherent kinase activity but serves as a dock for other well-known signaling and cytoskeletal proteins. The cytoplasmic tail of syndecan-4 is organized into three regions, designated as C1 (conserved, membrane proximal), V (variable central), and C2 (conserved, C-terminal) based on sequence homology among the four syndecan family members.[26,27] Several binding partners for each region have been identified for the domains in syndecan-4: C1 – Src, Fyn, syndesmos, and dynamin 2;[28,29] V – PKCα, α-actinin, syndesmos;[13,14,18,30,31] C2 – Post synaptic density protein 95; Drosophila Disc-large; zonula occludens-1 domain proteins such as synectin,[32] syntenin,[33] and calcium/calmodulin-dependent serine protein kinase.[34] Thus, signaling from the syndecan cytoplasmic domains feeds into or influences several critical cell subsystems, including classical signaling pathways associated with cell adhesion and cytoskeletal organization.

The cell adhesion assays show differences in distribution of syndecan-4 and cytoskeletal organization between HS+ and HS− podocytes. In HS+ cells, the HS associated with syndecan-4 facilitates the development of large clusters or 'pods' of syndecan-4-positive immunoreactivity at the periphery of podocytes (Figure 3a) during the interaction

with fibronectin. In the HS− podocytes, syndecan-4-positive 'pods' did not readily develop (Figure 3d), but instead smaller punctate clusters were observed. In turn, the relative diameter of the clusters seems to be directly related to cytoskeletal organization-stress fiber formation ('pods'/HS+) vs cortical actin (punctate/HS−). Previous *in vitro* studies have shown that the formation of stress fibers is directly dependent on the binding of syndecan-4 through its HS chains[35] to the heparin-binding domain of fibronectin. In turn, stress fiber formation is mediated by downstream signaling by PKCα to RhoA.[36] Our adhesion assay data from the HS+ podocytes is consistent with what is known regarding RhoA signaling, that is, the clustering of individual syndecan-4 into large multimeric aggregates[13,17] (Figure 4a) facilitating the formation of stress fibers (Figure 3b).

In the HS− cells, our studies show a twofold increase in syndecan-4 expression and a fourfold increase in PKCα activation. The increase in surface expression of syndecan-4 in HS− podocytes was unexpected and the mechanism by which this occurs is currently under investigation. However, the resultant enhanced activation of PKCα, because of a net increase in the amount of syndecan-4 present on the cell surface, is very consistent with the findings of Keum *et al.*[30] One would therefore surmise that at the conclusion of the adhesion assay the HS− podocytes should have shown even more pronounced stress fiber formation. Our data showed the converse, suggesting that enhanced Rac1 activation was occurring in HS− podocytes, because the formation of cortical actin networks (Figure 3e) has been attributed to Rac1 activation rather than enhanced RhoA activation. Bass *et al.*[37] have shown that cell adhesion on intact fibronectin led to a differential timecourse for Rac1 and RhoA activation, with rapid activation of Rac1 ($\sim T = 30$ min) after cell attachment that persisted for 90 min. RhoA activity was initially suppressed ($\sim T = 30$ min) followed by subsequent activation at 120 min. Plating syndecan-4 null cells on fibronectin did not show a similar activation timecourse for Rac1 activation. Instead the syndecan-4 null cells showed an overall enhanced Rac1 activity, implicating a negative regulatory role of syndecan-4 in modulating Rac1 activation,[37]that is, the engagement of syndecan-4 by matrix ligands would initiate a decrease in Rac1 activity with the eventual progression toward RhoA activation. Cortical actin organization was previously reported in xylosyltransferase-deficient cells (CHO-745,[38]) which were also unable to assemble HS chains. Stress fiber formation was rescued in those cells by overexpressing a syndecan-4 construct,[38] the investigators suggesting that the non-glycanated syndecan-4 core protein was capable of mediating similar adhesive interactions by itself. However the cell–matrix interactions of the non-glycanated syndecan-4 core protein were less efficient because the rate of development of stress fibers was delayed from that observed in wild-type CHO-KI cells.[38] Our findings are consistent with the results of Echtemeyer *et al.*[38] because the HS− podocytes eventually assemble stress fibers within 24 h after seeding on fibronectin matrix but enhanced organization of cortical actin still persists in those cells (data not shown).

It is tempting to speculate that the observed upregulation in the surface expression of syndecan-4 with the concomitant upregulation of PKCα signaling could represent one aspect of an adaptive response by evoked by the podocyte to maintain cell–matrix interactions. This may be true for cells that are acting in a singular manner, but extrapolation of this speculative 'adaptive response' to what actually occurs *in vivo* seems may not be entirely accurate when one reconciles the observations seen for syndecan-4 staining in confluent podocyte monolayers (Figure 7) and animal models (Figure 8a cf Figure 8e). In the latter models, the level of staining intensity for syndecan-4 is directly correlative to the presence or absence of HS. There are several possible explanations for the loss of syndecan-4 core protein staining observed in HS null podocytes. One possibility is based in the difference in the size of the focal adhesions observed *in vitro* between the HS+ and HS− podocytes. It may be that the loss of HS from podocytes *in vivo* does result in a shift from larger 'pods' of syndecan 4 (Figure 3a) to diffusely distributed small clusters of syndecan-4 similar to that observed *in vitro* (Figure 3d). A second possible explanation could be that the lack of HS chains might render the syndecan-4 core protein more susceptible to proteolytic cleavage from the cell surface. It has been shown in other systems that the ectodomains of cell surface proteoglycans can be proteolytically removed from cell surfaces through the routine activities of 'sheddase' proteases, many of which fall within the matrix metalloproteinase family.[39] Some of these 'sheddases' are inhibited by tissue inhibitor of matrix metalloproteinases,[39] which is known to bind HS.[40,41] In wild-type podocytes, the HS chains could serve to bind and localize protease inhibitors such as tissue inhibitor of matrix metalloproteinases to the immediate pericellular domain to protect the syndecan core proteins from degradation. The loss of HS would render the proteoglycan core protein susceptible to cleavage and release from the cell surface, which in turn, would dramatically affect cell adhesion.[42] Both scenarios are highly feasible and experiments are ongoing to discern which process might occur in this system.

This current report serves to highlight the fact that significant gaps in our understanding of podocyte glycobiology still exist and that HS and their respective proteoglycan core proteins still have a definitive, critical role in glomerular biology. The podocyte 'interactome' that is regulated by the ligand-specific engagement of HS and their proteoglycan core protein tethers is far more complicated than what we have described in this initial report. Although in the present report, we applied the observation of the engagement–disengagement of syndecan-4 core protein to our model to highlight the importance of HS in modulating PKCα signaling and stress fiber formation, the homeostasis of the podocyte will certainly depend on the simultaneous engagement of multiple members of the syndecan family. There is no doubt, as with integrins, that normal podocyte adhesion and signaling mediated by the engagement of syndecans will

be the result of the integration of signaling and cytoskeletal organization from one or more sites along the cytoplasmic domain. Further studies in our laboratory to dissect the downstream signaling events leading from HS by syndecan core proteins to both the cytoskeleton and slit diaphragm are currently in progress.

MATERIALS AND METHODS

Animals and animal care

The characterization of the PEXTKO mouse model was reported previously.[4] Mice were housed under controlled light and humidity conditions in the LSU Health Sciences Center Animal Resource Facility, an approved facility by the Association for Assessment and Accreditation of Laboratory Animal Care. All experimentation followed the guidelines set down by the Association. Food and water was made freely available. Kidneys harvested from age-matched 2.5P-Cre/Agrn +/fl and 2.5P-Cre/Agrn fl/fl mice were a generous gift of Dr Jeffrey Miner, Department of Medicine, Washington University, St Louis, MO, USA.

Development of immortalized *Ext1*$^{fl/fl}$ cell lines

To examine the role of cell surface PGs in mediating podocyte behavior, we bred the Immortomouse (H2Kb-tsA58 mouse, Charles River, Wilmington, MA, USA) with the *Ext1*$^{fl/fl}$ mice to eventually obtain H2Kb-tsA58/*Ext1*$^{fl/fl}$ genotype. Verification of correct genotype of weanling animals was carried out by PCR from tail snips using 5′-GGAGTGTGGATGAGTTGAAG-3′(forward) and 5′-CAACACTTTCAGCTCCAGTC-3′ (reverse) for *Ext1* as described previously[4] and 5′-AGCGCTTGTGTCGCCATTGTATTC-3′ (forward) and 5′-GTCACACCACAGAAGTAAGGTTCC-3′ (reverse) for the Immortomouse (according to the supplier's instructions). Cycling parameters for the Immortomouse PCR (as per the supplier's recommendations) were 94 °C 4 min; 94 °C 30 s, 58 °C 1 min, 72 °C 1.5 min, repeat 30 cycles; 72 °C 5 min. The resultant PCR products yield a 460 bp band for mice homozygotic for *Ext1*$^{fl/fl}$ and 1000 bp for the H2Kb-tsA58 transgene (Supplementary Figure S1). The immortomouse/*Ext1*$^{fl/fl}$ mice were viable and have been bred over 10 generations. Glomeruli were isolated from Immortomouse/*Ext1*$^{fl/fl}$ mice using a previously described magnetic separation protocol[43] adapted from Takemoto *et al.*[44] Immortalized *Ext1*$^{fl/fl}$ podocytes were isolated from glomerular explant cultures following previously published protocols[45] and cell lines were developed using limiting dilution methods. The cells were characterized by WT-1 and nestin staining as described.[43] *In vitro* excision of *Ext1* was conducted using adenoviral-mediated delivery of a green fluorescent protein-Cre recombinase construct; adenoviral delivery of a green fluorescent protein construct was used for control podocytes (Vector Biolabs, Philadelphia, PA, USA). Fluorescent-activated cell sorting was used to enrich for the virally transduced cell populations. Confirmation of the loss of HS copolymerase activity (*Ext1* inactivation) in green fluorescent protein-Cre-transfected cells was carried out by immunostaining with anti HS-GAG antibody HS4C3. Podocytes grown at 37 °C for >14 days in the absence of interferon γ were used for all adhesion and migration assays.

Cell adhesion and migration assays

Cell adhesion assays were carried out as described by Woods *et al.*[46] Briefly, podocytes were preincubated with cycloheximide (250 μg/ml) in serum-free medium (RPMI 1640 medium with 5 mmol/l glucose) for 2 h before the assay to inhibit endogenous synthesis of matrix molecules. Before seeding, a circular coverslip coated with fibronectin 100 μg/ml was placed at the bottom of wells in a 24-well plate and the well filled with serum-free medium containing cycloheximide. After preincubation, the cells were trypsinized, rinsed three times in serum-free medium, and resuspended in the same medium containing cycloheximide, and seeded into the wells in a 24-well plate at a concentration of 50,000 cells per well. For cell spread measures, the cells were seeded at 10,000 cells/well. Adhesion assays were run for 2 or 4 h. At the end of the adhesion assay, the cells were rinsed three times with phosphate-buffered saline (PBS) to remove unattached cells then fixed in 3.5% formaldehyde in PBS with 0.1% Tween-20. For adhesion assays using wild-type immortalized podocytes image acquisition was carried out at ×200 magnification, and 10 fields of view for each replicate within an assay was carried out, and a total of 50 cells were measured per replicate. For the subsequent adhesion assays with the HS+ and HS− podocytes image acquisition was carried out at ×20 (final magnification), which permitted the imaging of almost an entire well in one field of view. Cell number and spread cell areas were measured on digitized images using a planimetry subroutine in I-vision software (BioVision Technologies, Exton, PA, USA). The adhesion assays were run three times, with three replicates for each substrate condition.

For comparative studies, cells were harvested under identical conditions to those used in the flow cytometry studies (see below) and seeded onto fibronectin-coated substratum and subsequently fixed, stained, and imaged (see below) after 2 h of interaction with the substratum.

A scratch wound assay was used to detect potential differences in the migratory ability of HS+ and HS− podocytes to migrate. Briefly, a pipette tip was cut to give a working diameter of 1 mm. The tip was used to score a cross-shaped wound in confluent monolayers of differentiated podocytes grown in fibronectin-coated (100 μg/ml) 24-well plates. Registration marks (R – Figure 2a and b) flanking the wound were made on the underside of the plate to allow for alignment of photographic montages during analysis. Post-wounding, the wells rinsed with the medium three times to remove detached cells, and then fresh medium was added to the wells. This condition represented the $T=0$ point for the timecourse. The cells allowed to repair the wound for 48 h at 37 °C. Images were digitized for each well at $T=0$, 24, and 48 h using phase contrast microscopy at ×100 magnification. Image capture started at the center of the cross and moved laterally along the arms of the cross for at least four fields of view, taking care to overlap the edges of adjacent fields for compositing. Alignment of digitized images into larger montages was carried out using I-vision software. Each montage was subsequently overlaid in register with the other montages for its respective timecourse and cropped to the same sizes using Adobe Photoshop. Area measurements of the open wound were made from the cropped images using I-vision software. The area for each scratch wound was calculated using a planimetry subroutine in the image analysis software and the relative change in area from $T=0$ was determined using the equation $\frac{[A_o - A_n]}{A_o} = \Delta A$, where A_0 = area at $T=0$, A_n = area at Time = n, and ΔA is the relative change in area. Statistically significant differences between the groups were found using Student's *t*-test.

Immunohistochemistry and digital microscopy

Immunostaining of tissue sections from wild-type and PEXTKO mice and cell cultures was conducted using previously published methods.[4,43] Before staining, cell cultures were fixed with freshly

prepared 3.5% formalin in PBS with 0.1% Tween-20. Antibodies used in this study were anti-HS (HS4C3, TVK), a core protein-specific rat anti-mouse syndecan-4 monoclonal antibody (clone KY/8.2, BD Pharmigen, San Jose, CA, USA), rat anti-mouse perlecan (A7L6, Millipore, Billerica, MA, USA), rabbit anti-human vinculin (V4139, Sigma Chemical, St Louis, MO, USA), rabbit anti α-actinin-4 (42-1400, Zymed, South San Francisco, CA, USA), rabbit anti-PKCα (#2056, Cell Signaling Technology, Beverly, MA, USA), rabbit anti-synaptopodin (# 163002, Synaptic Systems, Goettingen, Germany), Texas Red (or Alexa-488)-conjugated phalloidin and Hoechst 333242 (Invitrogen, Carlsbad, CA, USA). For flow cytometry studies (see below), a phycoerythrin-conjugated syndecan-4 antibody (BD Pharmagen) was used. Species-specific secondary antibodies were purchased from Jackson Immunoresearch, Malvern, PA, USA and the anti-VSV antibodies purchased from Sigma (1:100, clone P5D4). Immunostained cultures were imaged using an Olympus IX-70 microscope (Olympus-America, Center Valley, PA, USA) equipped with epifluorescent illumination, the images digitized using a Hamamatsu Orca camera (Hamamatsu USA, Bridgewater, NJ, USA), the signal from which ported to a Macintosh PowerPC hosting IVision imaging software.

Membrane fractionation and PKCα translocation assays

HS+ and HS− cells were seeded (160,000 cells per well) in serum-free medium into six-well plates that had been precoated with fibronectin as described above. After 4 h of incubation, the cells were washed once in ice-cold PBS and lysed in 300 µl buffer containing 20 mmol/l Tris pH 7.5, 2 mmol/l 2-mercaptoethanol, 5 mmol/l ethyleneglycol tetraacetic acid, 2 mmol/l ethylene-diaminetetraacetic acid, and 1X protease inhibitor cocktail (Sigma). Lysates were scraped, collected into microcentrifuge tubes, and spun for 30 min at 15,000 *g* at 4 °C. Supernatant was then collected as the cytosolic fraction. The remaining pellet was resuspended in 150 µl buffer containing 50 mmol/l Tris pH 8.0, 150 mmol/l NaCl, 1% NP-40, 10 mmol/l NaF, 2 mmol/l Na_3VO_4, and 1× protease inhibitor and spun for 30 min at 13,000 *g* at 4 °C. Supernatant was taken as the membrane fraction. The membrane and cytosolic fractions were analyzed for PKCα levels by western blotting. Total β1 integrin levels were determined for normalization and for verifying the efficiency of membrane fractionation, glyceraldehyde 3-phosphate dehydrogenase was used for normalization of intracellular PKCα levels.

Flow cytometry

Phycoerythrin-conjugated syndecan-4 antibodies (see above) or phycoerythrin-conjugated isotype-control (rat IgG2a, kappa, #554689, BD Biosciences, San Jose, CA, USA) were used for flow cytometry staining protocols according to the supplier's directions. Briefly HS+ and HS− podocytes were trypsinized and prepared as single cell suspensions in 10 ml complete medium and incubated in a waterbath at 37 °C for 2 h to allow for cell recovery after trypsination. Afterward, the cells were pelleted by low speed centrifugation and then resuspended in Dulbecco's PBS buffer (2.68 mmol/l KCl, 136.9 mmol/l NaCl, 1.46 mmol/l KH_2PO_4, 8.1 mmol/l Na_2HPO_4, pH 7.4, 1% heat-inactivated fetal bovine serum) at 1×10^7 cells/ml. All blocking and staining steps for the protocol were conducted at 37 °C because it was found the cells would spontaneously aggregate at 4 °C. In all, 100 µl aliquots of the cell suspension were blocked for 15 min with Mouse BD Fc Blocking Agent (#553141, BD Biosciences), used at a concentration of 0.125 µg $\times 10^6$ cells. Afterward, the cells were stained for 45 min with either the phycoerythrin-conjugated syndecan-4 antibody or the isotype-specific control antibody (0.25 µg/10^6 cells, the concentration predetermined based on antibody staining titration curves). Afterward, 300 µl of buffer was added to the cell suspension and the cells were pelleted by centrifugation. The cells were then resuspended and washed in 300 µl of buffer and again pelleted by centrifugation followed by a subsequent resuspension/wash step in 1.4 ml buffer. All data were collected using a BD LSR II flow cytometer (BD Biosciences) made available through the Research Core Facility at the Louisiana State University Health Sciences Center-Shreveport (Shreveport, LA, USA). The LSR II has a Coherent Sapphire laser for 488-nm excitation, a JDS Uniphase HeNe laser for 633-nm excitation, as well as a Coherent VioFlame for 405-nm excitation. Data analysis was performed using FACS Diva software (BD Bioscience) and FlowJo software (Tree Star, Ashland, OR, USA). Dead cells were excluded from analysis by forward and 90° laser light scatter properties and a minimum of 10,000 events was collected for each sample. Spectral overlap between the fluorochromes was compensated electronically based on single color control samples.

DISCLOSURE

All the authors declared no competing interests.

ACKNOWLEDGMENTS

Work on this project was funded in part by grants from the National Institutes of Health (1-RO1- DK077860-01A1 and 3R01DK077860-02S1, KJM). The authors wish to thank Ms Shannon Mumphrey of the LSU Health Science Center Research Core Facility for her assistance with the flow cytometry studies in this report. The authors also thank Jeffrey Miner, PhD (Washington University School of Medicine) for his gift of kidneys from control and podocyte-specific agrin knockout mice.

SUPPLEMENTARY MATERIAL

Figure S1. Agarose gel electrophoresis of PCR products from screening H2Kb-tsA58/*Ext1*$^{fl/fl}$ mice.
Supplementary material is linked to the online version of the paper at http://www.nature.com/ki

REFERENCES

1. Kanwar YS, Farquhar MG. Anionic sites in the glomerular basement membrane. *In vivo* and *in vitro* localization to the lamina rarae by cationic probes. *J Cell Biol* 1979; **81**: 137–153.
2. Kanwar YS, Linker A, Farquhar MG. Increased permeability of the glomerular basement membrane to ferritin after removal of glycosaminoglycans (heparan sulfate) by enzyme digestion. *J Cell Biol* 1980; **86**: 688–693.
3. Harvey SV, Jarad G, Cunningham J *et al.* Disruption of glomerular basement membrane charge through podocyte-specific mutation of agrin does not alter glomerular permselectivity. *Am J Path* 2007; **171**: 139–152.
4. Chen S, Wassenhove-McCarthy DJ, Yamaguchi Y *et al.* Loss of heparan sulfate glycosaminoglycan assembly in podocytes does not lead to proteinuria. *Kidney Int* 2008; **74**: 289–299.
5. Woods A. Syndecans: transmembrane modulators of adhesion and matrix assembly. *J Clin Invest* 2001; **107**: 935–941.
6. Woods A, Couchman JR. Syndecan-4 and focal adhesion function. *Curr Opin Cell Biol* 2001; **13**: 578–583.
7. Yung S, Woods A, Chan TM *et al.* Syndecan-4 up-regulation in proliferative renal disease is related to microfilament organization. *Faseb J* 2001; **15**: 1631–1633.
8. Cevikbas F, Schaefer L, Uhlig P *et al.* Unilateral nephrectomy leads to up-regulation of syndecan-2- and TGF-beta-mediated glomerulosclerosis in syndecan-4 deficient male mice. *Matrix Biol* 2008; **27**: 42–52.
9. Couchman JR, Woods A. Syndecan-4 and integrins: combinatorial signaling in cell adhesion. *J Cell Sci* 1999; **112**(Pt 20): 3415–3420.
10. Sweeney SM, Guy CA, Fields GB *et al.* Defining the domains of type I collagen involved in heparin- binding and endothelial tube formation. *Proc Natl Acad Sci USA* 1998; **95**: 7275–7280.

11. Ten Dam GB, Kurup S, van de Westerlo EM *et al.* 3-O-sulfated oligosaccharide structures are recognized by anti-heparan sulfate antibody HS4C3. *J Biol Chem* 2006; **281**: 4654–4662.
12. Woods A, Couchman JR. Syndecan 4 heparan sulfate proteoglycan is a selectively enriched and widespread focal adhesion component. *Mol Biol Cell* 1994; **5**: 183–192.
13. Choi Y, Kim S, Lee J *et al.* The oligomeric status of syndecan-4 regulates syndecan-4 interaction with alpha-actinin. *Eur J Cell Biol* 2008; **87**: 807–815.
14. Greene DK, Tumova S, Couchman JR *et al.* Syndecan-4 associates with alpha-actinin. *J Biol Chem* 2003; **278**: 7617–7623.
15. Roh YH, Kim YH, Choi HJ *et al.* Syndecan-1 expression in gallbladder cancer and its prognostic significance. *Eur Surg Res* 2008; **41**: 245–250.
16. Oh ES, Woods A, Lim ST *et al.* Syndecan-4 proteoglycan cytoplasmic domain and phosphatidylinositol 4,5-bisphosphate coordinately regulate protein kinase C activity. *J Biol Chem* 1998; **273**: 10624–10629.
17. Oh ES, Woods A, Couchman JR. Multimerization of the cytoplasmic domain of syndecan-4 is required for its ability to activate protein kinase C. *J Biol Chem* 1997; **272**: 11805–11811.
18. Oh ES, Woods A, Couchman JR. Syndecan-4 proteoglycan regulates the distribution and activity of protein kinase C. *J Biol Chem* 1997; **272**: 8133–8136.
19. Kanwar YS, Farquhar MG. Isolation of glycosaminoglycans (heparan sulfate) from glomerular basement membranes. *Proc Natl Acad Sci USA* 1979; **76**: 4493–4497.
20. Woods A, Hook M, Kjellen L *et al.* Relationship of heparan sulfate proteoglycans to the cytoskeleton and extracellular matrix of cultured fibroblasts. *J Cell Biol* 1984; **99**: 1743–1753.
21. Woods A, Couchman JR, Hook M. Heparan sulfate proteoglycans of rat embryo fibroblasts. A hydrophobic form may link cytoskeleton and matrix components. *J Biol Chem* 1985; **260**: 10872–10879.
22. Bass MD, Morgan MR, Roach KA *et al.* p190RhoGAP is the convergence point of adhesion signals from alpha 5 beta 1 integrin and syndecan-4. *J Cell Biol* 2008; **181**: 1013–1026.
23. Weinbaum S, Tarbell JM, Damiano ER. The structure and function of the endothelial glycocalyx layer. *Annu Rev Biomed Eng* 2007; **9**: 121–167.
24. Goldberg S, Harvey SJ, Cunningham J *et al.* Glomerular filtration is normal in the absence of both agrin and perlecan-heparan sulfate from the glomerular basement membrane. *Nephrol Dial Transplant* 2009; **24**: 2044–2051.
25. Laurie GW, Bing JT, Kleinman HK *et al.* Localization of binding sites for laminin, heparan sulfate proteoglycan and fibronectin on basement membrane (type IV) collagen. *J Mol Biol* 1986; **189**: 205–216.
26. Couchman JR, Chen L, Woods A. Syndecans and cell adhesion. *Int Rev Cytol* 2001; **207**: 113–150.
27. Morgan MR, Humphries MJ, Bass MD. Synergistic control of cell adhesion by integrins and syndecans. *Nat Rev Mol Cell Biol* 2007; **8**: 957–969.
28. Kinnunen T, Kaksonen M, Saarinen J *et al.* Cortactin-Src kinase signaling pathway is involved in N-syndecan-dependent neurite outgrowth. *J Biol Chem* 1998; **273**: 10702–10708.
29. Yoo J, Jeong MJ, Cho HJ *et al.* Dynamin II interacts with syndecan-4, a regulator of focal adhesion and stress-fiber formation. *Biochem Biophys Res Commun* 2005; **328**: 424–431.
30. Keum E, Kim Y, Kim J *et al.* Syndecan-4 regulates localization, activity and stability of protein kinase C-alpha. *Biochem J* 2004; **378**: 1007–1014.
31. Denhez F, Wilcox-Adelman SA, Baciu PC *et al.* Syndesmos, a syndecan-4 cytoplasmic domain interactor, binds to the focal adhesion adaptor proteins paxillin and Hic-5. *J Biol Chem* 2002; **277**: 12270–12274.
32. Gao Y, Li M, Chen W *et al.* Synectin, syndecan-4 cytoplasmic domain binding PDZ protein, inhibits cell migration. *J Cell Physiol* 2000; **184**: 373–379.
33. Zimmermann P, Tomatis D, Rosas M *et al.* Characterization of syntenin, a syndecan-binding PDZ protein, as a component of cell adhesion sites and microfilaments. *Mol Biol Cell* 2001; **12**: 339–350.
34. Cohen AR, Woods DF, Marfatia SM *et al.* Human CASK/LIN-2 binds syndecan-2 and protein 4.1 and localizes to the basolateral membrane of epithelial cells. *J Cell Biol* 1998; **142**: 129–138.
35. Longley RL, Woods A, Fleetwood A *et al.* Control of morphology, cytoskeleton and migration by syndecan-4. *J Cell Sci* 1999; **112**(Pt 20): 3421–3431.
36. Saoncella S, Echtermeyer F, Denhez F *et al.* Syndecan-4 signals cooperatively with integrins in a Rho-dependent manner in the assembly of focal adhesions and actin stress fibers. *Proc Natl Acad Sci USA* 1999; **96**: 2805–2810.
37. Bass MD, Roach KA, Morgan MR *et al.* Syndecan-4-dependent Rac1 regulation determines directional migration in response to the extracellular matrix. *J Cell Biol* 2007; **177**: 527–538.
38. Echtermeyer F, Baciu PC, Saoncella S *et al.* Syndecan-4 core protein is sufficient for the assembly of focal adhesions and actin stress fibers. *J Cell Sci* 1999; **112**(Pt 20): 3433–3441.
39. Fitzgerald ML, Wang Z, Park PW *et al.* Shedding of syndecan-1 and -4 ectodomains is regulated by multiple signaling pathways and mediated by a TIMP-3-sensitive metalloproteinase. *J Cell Biol* 2000; **148**: 811–824.
40. Woessner Jr JF. That impish TIMP: the tissue inhibitor of metalloproteinases-3. *J Clin Invest* 2001; **108**: 799–800.
41. Yu WH, Yu S, Meng Q *et al.* TIMP-3 binds to sulfated glycosaminoglycans of the extracellular matrix. *J Biol Chem* 2000; **275**: 31226–31232.
42. Rodriguez-Manzaneque JC, Carpizo D, Plaza-Calonge Mdel C *et al.* Cleavage of syndecan-4 by ADAMTS1 provokes defects in adhesion. *Int J Biochem Cell Biol* 2009; **41**: 800–810.
43. Lauer M, Scruggs B, Chen S *et al.* Leprecan distribution in the developing and adult kidney. *Kidney Int* 2007; **72**: 82–91.
44. Takemoto M, Asker N, Gerhardt H *et al.* A new method for large scale isolation of kidney glomeruli from mice. *Am J Pathol* 2002; **161**: 799–805.
45. Shankland SJ, Pippin JW, Reiser J *et al.* Podocytes in culture: past, present, and future. *Kidney Int* 2007; **72**: 26–36.
46. Woods A, Longley RL, Tumova S *et al.* Syndecan-4 binding to the high affinity heparin-binding domain of fibronectin drives focal adhesion formation in fibroblasts. *Arch Biochem Biophys* 2000; **374**: 66–72.